Postglacial denudation of western Tibetan Plateau margin outpaced by long-term exhumation

Henry Munack[a, *], Oliver Korup[a], Alberto Resentini[b], Mara Limonta[b], Eduardo Garzanti[b], Jan H. Blöthe[a], Dirk Scherler[a,c], Hella Wittmann[d], and Peter W. Kubik[e]

[a] Institute of Earth and Environmental Sciences, Universität Potsdam, 14476 Potsdam, Germany;
[*]Corresponding author: henry.munack@geo.uni-potsdam.de, +49 331 977 6272;
[b] Department of Earth and Environmental Sciences, Università degli Studi di Milano-Bicocca, 20126 Milano;
[c] Geological and Planetary Sciences, California Institute of Technology, Pasadena, CA 91125, USA;
[d] GFZ Deutsches GeoForschungsZentrum, 14473 Potsdam, Germany;
[e]Laboratory of Ion Beam Physics, ETH Zürich, 8093 Zürich, Switzerland

Here we provide data and additional figures concerning the petrographic analysis and the heavy minerals assemblages behind this study. Also, for the purpose of comparison, we show basin-wide ^{10}Be-derived denudation rates from various scaling schemes.

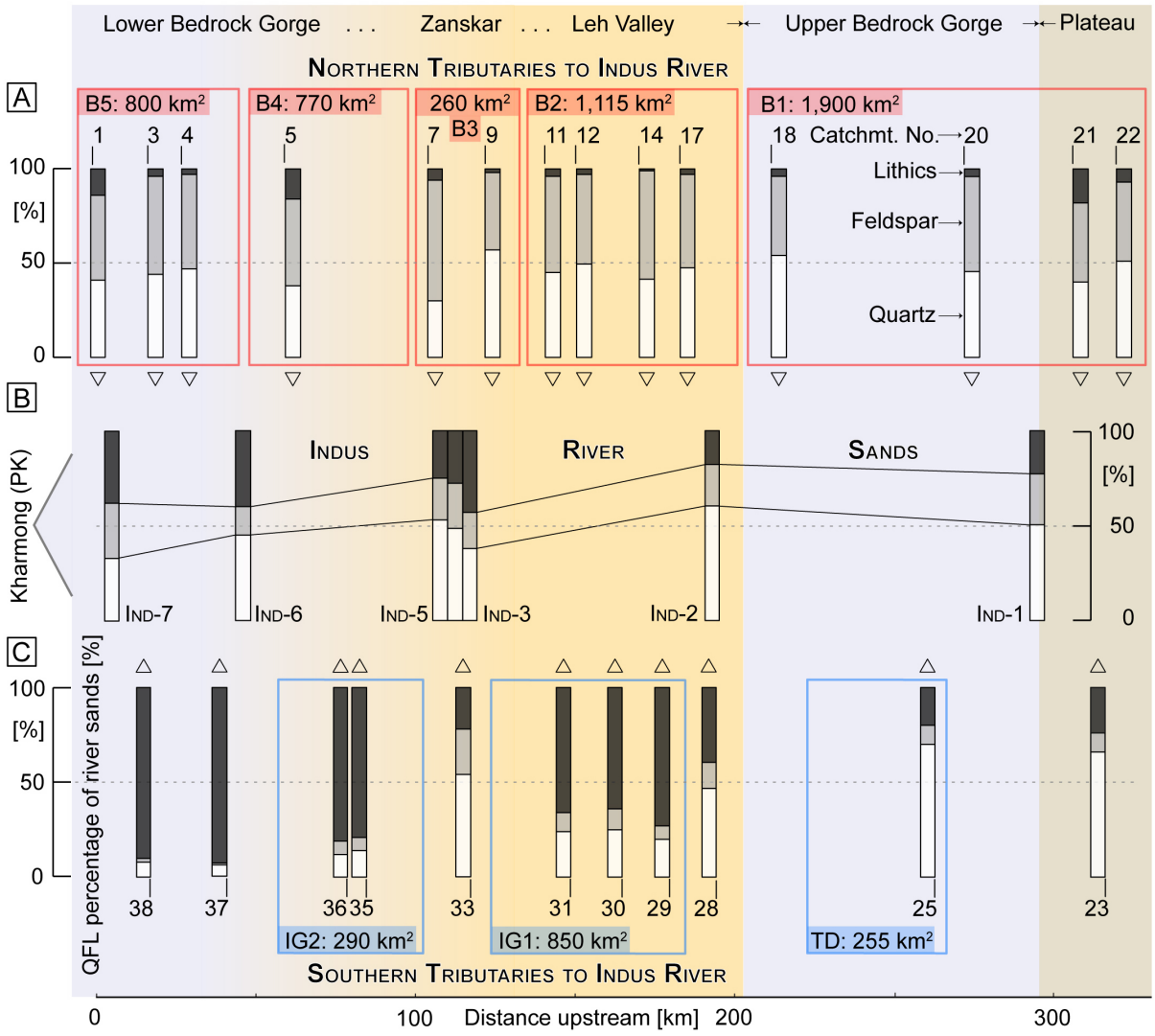

Figure DR1: Alternative to Fig. 4. Sand petrography in the upper Indus River catchment.

Figure DR1: Northern tributaries (draining the Ladakh Batholith) shed quartzo-feldspathic to feldspatho-quartzose detritus. Instead, southern tributaries (draining Indus Group siliciclastics and different tectonic units exposed along the ophiolitic suture and in the Zanskar Range to the south) shed abundant sedimentary, metasedimentary and locally metavolcanic, metabasite and ultramafite rock fragments. Provenance reaches denoted by frames are homogeneous units that were used to calculate relative sediment budgets (Red: B1–5 = Ladakh Batholith; Blue: TD = Tso Morari Dome, IG1–2 = Indus Group). Main southern tributaries (Gya (28), Zanskar (33), and Yapola (37) Rivers) represent distinct provenance reaches. Note stepwise increase in lithics (L) in Indus River sands downstream of the Gya confluence (IND-3) and of the Zanskar confluence (IND-6), due to prevailing IG1 and IG2 contribution. The opposite trend, observed locally at the Zanskar confluence, reflects prominent supply from the Zanskar Range (IND-4). Southern tributaries: catchments 23–25 mainly draining Tso Morari Dome; Gya (28), catchments 29–32 and 36 largely draining sedimentary Indus Group; Zanskar catchment largely draining sedimentary Tethys Himalaya Zone (THZ) and High Himalayan Crystalline Zone; Yapola (37) catchment largely draining THZ and Dras volcanics; and catchment (38) draining Dras volcanics.

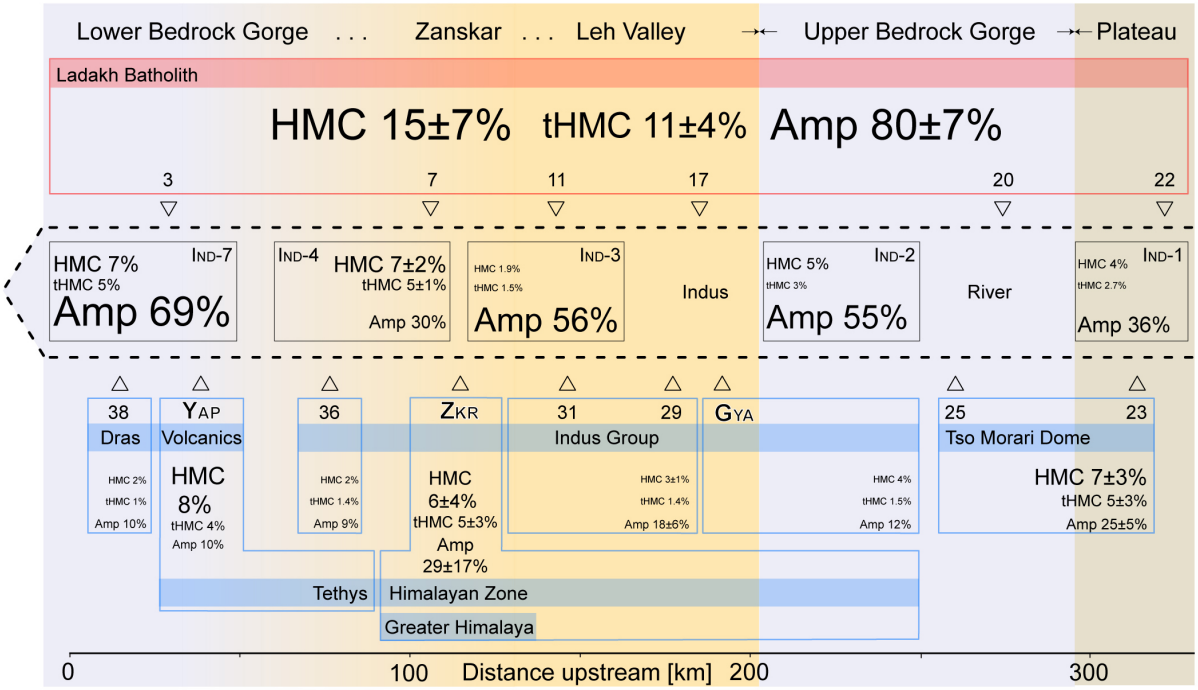

Figure DR2: Alternative to Fig. 5. Heavy minerals in the upper Indus River catchment. Font size is scaled proportionally to relative HM contribution to respective samples. YAP = Yapola River, ZKR = Zanskar River, GYA = Gya River; Amp = Amphibole, HMC = volume percentage of total, and tHMC = transparent heavy minerals (Garzanti and Andó, 2007). Note dilution of amphibole and HMC increase in Indus sands just after the Zanskar confluence. HMC (Heavy Mineral Concentration) classes are defined as follows: < 0.1 - extremely poor in Heavy Minerals; $0.1 \leq$ HMC < 0.5 - very poor; $0.5 \leq$ HMC < 1 - poor; $1 \leq$ HMC < 2 - moderately poor; $2 \leq$ HMC < 5 - moderately rich; $5 \leq$ HMC < 10 - rich; $10 \leq$ HMC < 20 - very rich. Provenance reaches as in Figure DR1.

Table DR1: Data from petrographic analysis.

No.	Sample (River)	Site	Components																			
						Lithic grains																
			Q	KF	P	Lvm	Lch	Lcc	Lcd	Lp	Lms	Lmf	Lmb	Lu	Mu	Bi	HM	total	MI[a]	Q	F	L
Northern Indus River tributaries (= Ladakh Batholith)																						
22	Nyoma	Nyoma	48	15	24	1	0	0	0	0	1	4	0	0	0	3	3	100	363	51	42	7
20	Chuma-1	Chumathang	36	10	30	0	0	0	0	0	0	3	0	0	0	1	20	100	379	45	50	4
18	Ligchi	Ligchi	44	11	23	0	0	0	0	0	0	3	0	0	4	4	12	100	393	54	42	4
17	Igoo	Igoo	41	15	29	0	0	0	0	0	0	2	0	0	0	5	7	100	428	48	50	3
14	Stagmo	Stagmo	29	7	33	0	0	0	0	0	0	1	0	0	2	7	21	100	456	41	57	1
12	Leh	Leh	39	14	24	0	0	0	0	1	0	1	0	0	0	8	12	100	420	50	48	3
11	Phyang	Phyang	34	9	29	0	0	0	0	0	0	2	1	0	0	5	19	100	391	45	51	4
9	Humla	Humla	38	8	19	0	0	1	0	0	0	1	0	0	1	6	27	100	444	57	41	2
7	Basgo	Basgo	27	17	41	1	1	1	0	1	1	1	0	0	1	1	9	100	NA	30	64	6
4	Domkar	Domkar	40	14	29	0	0	0	0	0	0	1	0	0	0	2	13	100	374	47	50	3
3	Skyur	Skurbuchan	40	12	35	0	0	1	0	0	0	1	1	0	1	3	4	100	400	44	52	4
Ladakh Batholith (+ Indus Group component)																						
21	Nogo	Nogo	38	10	30	0	0	1	0	11	3	2	0	0	0	1	3	100	204	40	42	18
5	Nurla	Nurla	31	6	31	0	0	0	0	6	6	1	0	0	0	3	15	100	133	38	46	16
1	Hanuthang	Hanuthang	35	10	28	0	0	3	1	1	3	2	1	0	1	2	12	100	344	41	45	14
Southern Indus River tributaries																						
Tsomorari Dome																						
23	Nidder	Nidder	54	3	5	0	0	3	1	2	7	6	1	1	6	2	10	100	291	66	10	24
25	Skid	Skid	62	4	4	0	0	0	0	1	1	14	1	1	8	2	3	100	345	70	10	20
Nyimaling Granite																						
28	Gya	Upshi	44	4	9	1	0	8	1	12	11	2	1	1	0	0	6	100	114	47	14	39
Indus Group																						
29	Martse	Martselang	19	2	5	1	0	5	0	51	13	0	0	0	0	0	2	100	28	20	7	73
30	Matho	Matho	25	2	9	0	0	3	0	38	22	0	0	0	0	0	1	100	50	25	11	64
31	Stok	Stok	24	2	8	2	0	3	0	42	19	0	1	0	0	0	0	100	47	24	10	66
Zanskar catchment																						
33	Zanskar	pre Indus	48	11	11	0	0	10	3	0	1	4	1	0	3	5	3	100	NA	54	24	22
33.2	Zanskar	post Sumdah	43	5	8	1	0	22	3	0	2	2	1	0	0	1	11	100	337	49	15	36
33.1	Zanskar	pre Markha	42	3	8	0	0	24	5	0	2	3	0	0	0	1	10	100	332	48	12	40
33.01	Markha	pre Zanskar	23	1	2	0	0	44	2	6	12	5	0	3	0	0	2	100	155	23	3	74
Indus Group																						
35	Lardo	Lardo	14	1	6	4	0	2	0	28	44	0	0	0	0	0	1	100	80	14	7	79
36	Giera	Giera	12	1	6	2	0	14	0	27	35	0	0	2	0	0	1	100	70	12	7	81
Spontang Ophiolite																						
37	Yapola	Kalshi	5	0	1	1	0	46	6	14	12	0	2	10	0	0	3	100	86	6	1	93
Dras-Nidam volcanics																						
38	Leido	Leido	8	0	1	1	0	9	1	26	40	0	0	12	0	0	1	100	70	8	2	91
Trunk Indus River																						
	LAT [°N]	LON [°E]																				
Ind-1	33.26613	78.48705	46	11	13	1	1	4	2	0	5	5	0	2	2	1	6	100	236	51	27	23
Ind-2	33.80973	77.83070	56	8	12	2	0	4	1	0	3	4	0	3	3	1	5	100	250	61	22	18
Ind-3	34.16052	77.33836	36	6	12	1	0	5	2	21	8	2	1	1	1	2	3	100	NA	38	19	43
Ind-4	34.18390	77.33632	45	11	11	0	0	10	3	4	3	5	1	0	1	2	4	100	NA	49	24	28
Ind-5	34.20691	77.29174	48	8	12	0	0	15	3	1	2	2	0	0	1	4	6	100	262	53	22	25
Ind-6	34.31893	76.88656	40	4	9	1	0	22	3	4	4	2	0	0	1	3	6	100	157	45	15	40
Ind-7	34.54000	76.61967	28	10	15	0	0	14	1	7	5	3	0	2	0	5	8	100	226	33	29	38

Q - Quartz; KF - K-feldpar; P - Plagioclase; Lithic grains: Lvm - Volcanic and Metavolcanic, Lch - Chert, Lcc - Limestone, Lcd - Dolostone, Lp - Shale/Siltstone/Sandstone, Lms - Metasedimentary, Lmf - Felsic Metamorphic (med. and hi. rank), Lmb - Mafic Metamorphic (med. and hi. rank), Lu - Ultramafic (serpentinite), Mu - Muscovite, Bi - Biotite, HM - Heavy Minerals (as determined from petrographic point counting), MI - Metamorphic Index [a] (Garzanti et al., 2010; Garzanti and Vezzoli, 2003). Samples range from upper-very-fine sand to upper-medium sand (3.5 to 1 ϕ); grain size was determined by ranking and direct measurement in thin section.

Table DR2: Heavy Minerals assemblages derived from river sands that were also used for *in-situ* ^{10}Be analysis and petrographic analysis.

No.	HM% VFS-FS	HM% trp	% trp	% opq	% tbd	Zrn	Tur	Rt	Ttn	Ap	Brt	Ep	Grt	St	And	Sil	Hbl	Na-Amp	Amp	Cpx	En	Hyp	Ol	Spl	HCI	MMI	SI	ZTR
Northern Indus River tributaries (= Ladakh Batholith)																												
22	4	3	80	4	16	1	1	1	2	4	0	7	1	0	0	0	72	0	3	6	0	2	1	0	15	NA	NA	3
21	16	14	82	6	12	0	1	0	3	2	0	10	1	0	0	0	76	0	1	4	0	0	0	0	5	NA	NA	1
17	5	4	88	6	6	1	0	0	7	5	0	6	0	0	0	0	79	0	0	0	0	0	0	0	4	NA	NA	2
11	22	12	57	35	8	4	1	0	6	2	0	4	0	0	0	0	65	0	4	7	0	5	0	0	14	NA	NA	5
7	20	13	63	29	8	1	0	0	2	1	0	6	1	0	0	0	82	0	0	3	0	2	0	0	16	NA	NA	1
3	14	12	82	7	11	0	0	0	6	1	0	2	0	0	0	0	88	0	1	1	0	0	0	0	10	NA	NA	0
Southern Indus River tributaries																												
Tsomorari Dome																												
23	10	7	67	2	31	1	1	2	1	6	0	13	36	0	0	0	1	21	6	8	0	1	2	0	NA	NA	NA	4
25	5	3	56	6	38	4	5	1	1	14	0	10	33	0	0	1	8	12	1	5	0	0	0	0	8	NA	NA	11
Nyimaling Granite																												
28	4	1.5	36	14	51	9	7	2	3	5	0	53	6	0	0	0	11	0	1	1	0	0	0	3	5	NA	NA	18
Indus Group																												
29	4	1.4	33	6	60	3	2	0	1	3	0	65	8	0	0	0	13	0	1	0	0	0	0	1	6	NA	NA	6
31	3	1.4	46	6	48	2	0	0	1	1	0	66	4	0	0	0	20	0	2	1	0	0	0	0	12	NA	NA	3
Zanskar catchment																												
33	4	3	95	2	3	3	9	1	2	0	0	7	10	1	0	21	39	0	2	4	0	0	0	0	22	96	2	13
33.1	9	7	82	4	14	3	2	0	2	3	0	3	31	0	0	32	16	1	0	4	0	0	0	0	26	99	14	5
33.01	4	0.7	15	9	76	8	11	0	1	8	2	31	8	0	0	0	2	0	19	8	0	0	0	0	NA	NA	NA	20
Indus Group																												
36	2	1.4	67	1	32	2	1	0	0	1	0	76	4	0	2	1	7	0	1	2	0	0	0	0	24	67	NA	4
Spontag Ophoilite																												
37	8	4	46	3	51	0	0	0	0	0	0	20	0	0	0	0	0	0	0	7	14	0	55	2	NA	NA	NA	0
Dras-Nidam Volcanics																												
38	2	0.9	48	3	49	0	1	0	0	1	0	18	1	0	0	0	8	0	2	69	1	0	0	1	7	NA	NA	1
Trunk Indus River																												
Upstream Indus-Zanskar confluence																												
IND-1	4	3	60	8	32	3	2	1	5	6	0	10	18	0	0	0	18	12	5	13	1	0	2	0	15	NA	NA	6
IND-2	5	3	57	4	39	0	3	1	2	2	0	21	10	0	0	0	32	20	3	4	0	0	0	0	5	NA	NA	5
IND-3	1.9	1.5	78	11	11	2	3	0	2	0	0	29	3	0	0	0	56	0	0	3	0	0	0	1	2	NA	NA	5
Downstream Indus-Zanskar confluence																												
IND-4	7	6	86	10	4	4	2	0	2	0	0	8	39	1	0	10	28	0	2	3	0	0	0	0	23	96	0	7
IND-5	4	4	87	5	8	1	1	0	4	2	0	2	15	0	0	27	42	0	2	1	0	0	0	0	13	100	43	3
IND-6	10	7	68	17	15	3	3	1	4	4	0	6	24	0	0	19	31	0	0	3	0	0	0	0	17	100	10	7
IND-7	7	5	74	10	16	1	3	0	2	5	0	9	4	0	0	5	55	9	5	5	0	1	0	0	7	100	56	3

HM% VFS-FS - Percentage of Heavy Minerals in the very-fine to fine sand class (63 - 250 μm); HM% transp. - Percentage of transparent Heavy Minerals, %trp (transparent) + %opq. (opaque) + %tbd (turbid) = 100%.

The following HM percentages sum up to a total of 100%:
Zrn - Zircon; Tur - Tourmaline; Rt - Rutile; TiO - Ti Oxides*; Ttn - Titanite; Ap - Apatite; Mnz - Monazite*; Brt - Barite; Ep - Epidote; Grt - Garnet;
Cld - Chloritoid (Cld (not in Table) was detected in the samples 33 and Ind-1 with 1%, respectively); St - Staurolite; And - Andalusite; Ky - Kyanite*; Sil - Sillimanite;
Hbl - Hornblende; Na-Amp - Na Amphibole; Amp - Amphibole; Cpx - Clinopyroxene; En - Enstatite; Hyp - Hypersthene; Ol - Olivine; Spl - Spinel; * HM not detected.

HCI - Hornblende Colour Index; MMI Metasedimentary Minerals Index (Andó et al., 2013); SI - Sillimanite Index;
ZTR - Percentage of chemically ultrastable mineral species (Zrn, Tur, Rt) among transparent detrital HM.

Table DR3: Denudation rates and uncertainties from different scaling schemes.

No.	Sample ID	**Denudation rate** - De (mm kyr^{-1})	**Uncertainty** dDe (1-σ level) (mm kyr^{-1})	**Denudation rate** - Du (mm kyr^{-1})	**Uncertainty** dDu (1-σ level) (mm kyr^{-1})	**Denudation rate** - Li (mm kyr^{-1})	**Uncertainty** dLi (1-σ level) (mm kyr^{-1})	**Denudation rate** - Lm (mm kyr^{-1})	**Uncertainty** dLm (1-σ level) (mm kyr^{-1})	**Denudation rate** - St (mm kyr^{-1})	**Uncertainty** dSt (1-σ level) (mm kyr^{-1})
Northern Indus River tributaries (= Ladakh Batholith)											
1	Hanu	103.06	12.17	99.66	11.71	105.64	10.68	99.48	8.81	99.20	9.01
2	Achina	66.11	7.73	65.07	7.57	68.15	6.78	62.91	5.45	61.24	5.44
3	Skyur	94.74	11.57	91.96	11.18	97.25	10.29	90.86	8.53	90.20	8.65
4	Domkar	73.83	8.72	72.42	8.51	76.07	7.68	69.61	6.14	68.13	6.16
5	Nurla	38.50	4.53	38.68	4.53	40.04	4.00	35.18	3.06	33.01	2.94
6	Saspo	45.02	5.31	45.02	5.29	46.74	4.69	41.17	3.59	38.99	3.49
7	Bazgo									38.53	8.00
8	Nimu	36.33	4.32	36.53	4.32	37.81	3.83	33.31	2.94	31.13	2.81
8.1	Nimu-11	34.02	4.08	34.30	4.10	35.43	3.64	31.16	2.80	28.95	2.66
9	Humla	21.24	2.53	21.62	2.57	22.24	2.25	19.26	1.70	17.43	1.57
10	Tharu	24.77	2.95	25.19	2.99	25.93	2.63	22.18	1.95	20.22	1.83
11	Phyang	28.35	3.37	28.75	3.40	29.62	2.99	25.41	2.23	23.35	2.10
12	Leh										
13	Sabu									20.09	2.80
14	Stagmo	20.03	2.40	20.50	2.45	21.02	2.14	17.72	1.57	15.93	1.45
15	Nang	28.53	3.38	28.87	3.41	29.79	3.00	25.91	2.27	23.83	2.14
16	Karu									20.08	2.80
17	Igoo	26.48	3.14	26.86	3.18	27.69	2.79	24.02	2.11	21.97	1.97
18	Ligchi	32.67	3.88	33.09	3.92	34.14	3.45	28.97	2.54	26.75	2.41
19	Kumdo	91.17	10.72	88.87	10.40	93.91	9.40	84.82	7.38	83.77	7.48
20	Chuma-1	31.39	3.74	31.91	3.78	32.87	3.33	27.46	2.41	25.23	2.27
21	Nogo	14.72	1.79	15.27	1.85	15.55	1.60	12.47	1.12	10.90	1.01
22	Nyoma	17.11	2.07	17.69	2.13	18.05	1.85	14.56	1.30	12.84	1.18
Southern Indus River tributaries											
23	Nidder	33.65	4.00	34.02	4.03	35.20	3.56	30.10	2.64	27.75	2.50
24	Chuma-2	10.85	1.33	11.28	1.37	11.48	1.19	9.26	0.84	7.94	0.74
25	Skid	33.47	3.97	33.90	4.00	35.01	3.53	29.62	2.59	27.33	2.45
26	Tiridoo	30.80	3.67	31.20	3.70	32.22	3.26	27.46	2.41	25.23	2.27
27	Tarch	38.67	4.57	38.87	4.57	40.28	4.05	35.12	3.06	32.82	2.93
28	Gya										
29	Martse	93.69	11.37	90.87	10.97	96.16	10.09	90.67	8.42	89.90	8.53
30	Matho	74.29	8.69	72.76	8.47	76.54	7.63	70.76	6.15	69.24	6.17
31	Stok-3	73.28	8.59	71.84	8.38	75.53	7.55	69.38	6.04	67.81	6.05
31.1	Stok-11	84.66	9.88	82.53	9.58	87.09	8.65	80.63	6.96	79.47	7.04
32	Zin	72.96	8.61	71.45	8.39	75.11	7.59	70.11	6.20	68.58	6.21
33	Zanskar										
34	Alchi	66.06	7.72	64.94	7.55	68.08	6.78	63.43	5.51	61.71	5.49
35	Lardo	81.22	9.60	79.26	9.32	83.52	8.46	77.99	6.92	76.77	6.97
36	Giera	115.93	14.20	111.54	13.59	118.55	12.63	113.85	10.81	114.14	11.07
37	Yapola										
38	Leido	107.15	13.39	103.38	12.85	109.47	12.01	107.26	10.59	107.28	10.80

Scaling schemes: Time-dependent - De (Desilets et al., 2006), Du (Dunai, 2001), Li (Lifton et al., 2005), Lm (Lal, 1991; Nishiizumi et al., 1989; Stone, 2000);
Time-independent - St (Lal, 1991; Stone, 2000).
Also see CRONUS online calculator for scaling schemes and reference production rates ((Balco et al., 2008); http://hess.ess.washington.edu/).
Denudation rates for Bazgo, Sabu and Karu catchments taken from Dortch et al. (2011); there labelled BWR-5 (Sabu), BWR-6 (Karu) and BWR-14 (Bazgo).

References

Andó, S., Morton, A., and Garzanti, E., 2013, Metamorphic grade of source rocks revealed by chemical fingerprints of detrital amphibole and garnet., *in* Scott, R., Smyth, H., Morton, A., and Richardson, N., eds., Sediment provenance studies in hydrocarbon exploration and production: Geological Society of London.

Balco, G., Stone, J.O., Lifton, N.A., and Dunai, T.J., 2008, A complete and easily accessible means of calculating surface exposure ages or erosion rates from 10Be and 26Al measurements: Quaternary Geochronology, v. 3, no. 3, p. 174–195.

Desilets, D., Zreda, M., and Prabu, T., 2006, Extended scaling factors for in situ cosmogenic nuclides: New measurements at low latitude: Earth and Planetary Science Letters, v. 246, no. 3-4, p. 265–276.

Dortch, J.M., Owen, L.A., Schoenbohm, L.M., and Caffee, M.W., 2011, Asymmetrical erosion and morphological development of the central Ladakh Range, northern India: Geomorphology, v. 135, no. 1-2, p. 167–180.

Dunai, T.J., 2001, Influence of secular variation of the geomagnetic field on production rates of in situ produced cosmogenic nuclides: Earth and Planetary Science Letters, v. 193, no. 1, p. 197–212.

Garzanti, E., and Andó, S., 2007, Heavy Mineral Concentration in Modern Sands: Implications for Provenance Interpretation: Developments in Sedimentology, v. 58, p. 517–545.

Garzanti, E., Resentini, A., Vezzoli, G., Andó, S., Malusà, M.G., Padoan, M., and Paparella, P., 2010, Detrital Fingerprints of Fossil Continental-Subduction Zones (Axial Belt Provenance, European Alps): The Journal of Geology, v. 118, no. 4, p. 341–362.

Garzanti, E., and Vezzoli, G., 2003, A Classification of Metamorphic Grains in Sands Based on their Composition and Grade: Research Methods Papers: Journal of Sedimentary Research, v. 73, no. 5, p. 830–837.

Lal, D., 1991, Cosmic ray labeling of erosion surfaces: in situ nuclide production rates and erosion models: Earth and Planetary Science Letters, v. 104, no. 2-4, p. 424–439.

Lifton, N.A., Bieber, J.W., Clem, J.M., Duldig, M.L., Evenson, P., Humble, J.E., and Pyle, R., 2005, Addressing solar modulation and long-term uncertainties in scaling secondary cosmic rays for in situ cosmogenic nuclide applications: Earth and Planetary Science Letters, v. 239, no. 1-2, p. 140–161.

Nishiizumi, K., Winterer, E.L., Kohl, C.P., Klein, J., Middleton, R., Lal, D., and Arnold, J.R., 1989, Cosmic ray production rates of 10Be and 26Al in quartz from glacially polished rocks: Journal of Geophysical Research, v. 94, no. B12, p. 17,907.

Stone, J.O., 2000, Air pressure and cosmogenic isotope production: Journal of Geophysical Research, v. 105, no. B10, p. 23,753–23,759.